Supplementary Information (SI) for Physical Chemistry Chemical Physics.
This journal is © the Owner Societies 2026

Supplementary Information for Field-nanoconfinement coupling enhanced water desalination in carbon nanotubes

Hangtong Li
College of Environmental and Resource Sciences, Zhejiang University,
866 Yuhangtang Rd., Hangzhou 310058, Zhejiang, China and
Key Laboratory of Coastal Environment and Resources of Zhejiang Province (KLaCER),
School of Engineering, Westlake University,
600 Dunyu Rd., Hangzhou 310030, Zhejiang, China

Zhuan Ge*
School of Physics, Chengdu University of Technology,
1 Erxianqiao East Third Rd., Chengdu 610059, Sichuan, China

Jihao Liu
Department of Mathematics with Computer Science,
Guangdong Technion-Israel Institute of Technology,
241 Daxue Rd, Shantou 515063,
Guangdong, China

Sergio Andres Galindo-Torres†
Key Laboratory of Coastal Environment and Resources of Zhejiang Province (KLaCER),
School of Engineering, Westlake University,
600 Dunyu Rd., Hangzhou 310030, Zhejiang, China

This Supplementary Information document provides detailed information regarding the methods and additional analyses supporting the findings presented in the main text. The content includes:

- **Simulation Setups and Computational Details:** A comprehensive description of the simulation setups and computational approaches used, including simulation parameters and specific methodologies.
- **Hydration Energy Calculations:** Detailed methodology for calculating the hydration energy, including relevant simulation methods and result verifications.
- **Potential of Mean Force Derivations and Calculation Methods:** The details of the computational approach and validity of the potential of mean force (PMF), with full derivations of the associated equations.
- **Molecular Orientation Analyses:** The methods used to analyze molecular orientations within the simulation, including any relevant metrics and techniques.
- **Supplementary Tables and Figures:** Data tables and figures that further substantiate the main text, including additional results and analyses that provide deeper insights into the study.

These information are provided to offer transparency and to enable credibility of the methods and results presented in the manuscript.

- Filename: Supplementary Information.pdf

I. METHOD

A. Modeling Establishment and Simulation Methods

An atomistic model for electric field-dependent reverse osmosis (RO) desalination was employed, comprising water molecules, sodium ions, chloride ions, two graphene sheets, and a single-wall carbon nanotube (SWCNT). As depicted in Fig. S1, the rigid CNT, with

---

[*] gezhuan@cdut.edu.cn

[†] s.torres@westlake.edu.cn

open ends connecting water reservoirs, simulated a nanochannel with an atomically smooth surface. The two reservoirs had dimensions of 5.2 nm × 5.3 nm × 4.0 nm. The CNT was modeled as rigid with fixed carbon atoms, so the thermostat was applied to the fluid rather than the solid wall. Since nanoconfined water exhibits similar properties in both rigid and flexible CNTs,[1] and the mean flow rates differ by only 10∼20%, a rigid CNT was selected to simplify the simulations [2–4]. Initially, the empty rigid CNTs with different chiralities were immersed in a large water box, where they were gradually filled with water under conditions of 298 K temperature and 1 atm pressure to generate the initial models. Once stability in the water density within the tube was reached, we calculated the number of water molecules present to determine the equilibrium density under these conditions. The measured cross-sectional snapshot of water molecules within the CNTs is consistent with previous studies.[5] The CNT within the model was filled with water molecules with the known number of water molecules derived before (nanoconfined liquid), and then the membrane was then immersed in the center of two 0.5 M NaCl solutions, which is slightly lower than the concentration of seawater (∼ 0.6 M). The two side reservoirs were designated as the feed and product reservoirs, with the membrane channel (CNT) serving as the conduit for solution-solvent separation between the two.

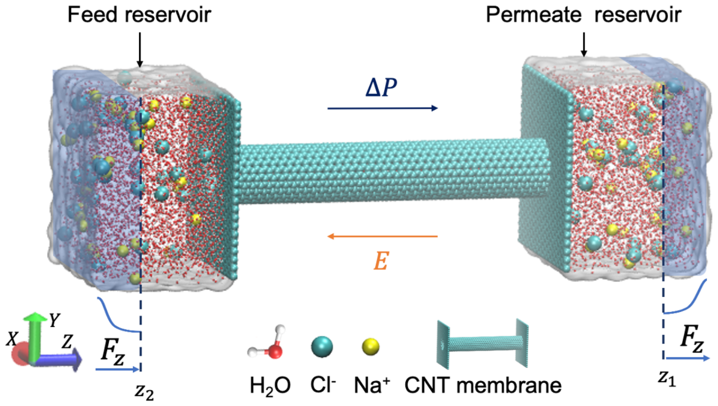

Fig. S1. Reverse osmosis (RO) desalination model under external electric fields. The model system consisting of a CNT embedded in two monolayer graphene sheets shown in cyan blue and separates the salt water across the membrane. Na^+ ions and Cl^- ions in the water are shown as yellow balls and cyan-blue particels, respectively. Water molecules are shown as transparent liquid for clarity. The force F_z is applied on the left reservoir to push the salt water across CNTs and F_z is also applied on the right reservoir to maintain the pressure difference ΔP.

The dimensions of the simulation box were 5.5 nm in the x- and y-directions and 18.0 nm in the z-direction, where the pressure gradient along the z-direction, with the applied electric field oriented along the negative z-direction at the same time. According to reports from Borg *et al.* [6] and Li *et al.* [7], the controllable pressure differences are generated by applying a Gaussian-distributed force to a specific area at both ends of the reservoirs in a model with periodic boundary conditions. This method has been demonstrated to facilitate pressure-driven nanoflow simulations while reducing simulation costs. [6, 7] As illustrated in Fig. S1, this represents the initial system setup snapshot in our simulations. The solution in the blue shadow area of the reservoirs was applied to a Gaussian distributed force $F_Z(z)$ from z = Z_1 to z = Z_2 crossing the periodic boundary, the magnitude of which was set to produce the pressure differences required in the simulations,

$$\Delta P = \rho_n \int_{Z_2}^{Z_1} F_Z(z)dz \tag{S1}$$

where ρ_n is the instantaneous number density. The Gaussian distributed force $F_Z(z)$ is the force applied to each water molecule in the z-direction:

$$F_Z(z) = \begin{cases} \overline{F}\exp(-(z-\alpha)^2/(2\nu_s^2)) & z_1 \leq z \leq z_2 \\ 0 & \text{otherwise} \end{cases} \tag{S2}$$

where $\overline{F}$ is the peak value of the Gaussian distributed force at the position α (i.e. the peaks are located at both ends of the two reservoirs, namely the center of the Gaussian distribution) and ν_s is the standard deviation of the Gaussian distribution that is smaller than the distance between Z_1 and Z_2. Then Eq. S2 is substituted for Eq. S1, we have gotten axial pressure difference ΔP between the feed reservoir and permeate reservoir from 200 to 400 MPa, which induces the pressure gradient to drive fluid transport transport CNTs. The nonequilibrium simulations were carried out in NVT ensemble for 10 ns where external pressures were applied, and the average pressures P_{feed} and $P_{permeate}$ of the feed reservoir and permeate reservoir are measured during the last 5 ns. P_{feed} and $P_{permeate}$ defined as the mean pressure calculated over the region excluding the areas where external mechanical forces were applied at the boundaries. The pressure differences and flow fields of the nanoconfined seawater transports were produced. For the RO desalination simulations, we employed the above-described setup to measure molecular properties and evaluate desalination performance under an applied electric field.

B. Hydration energy calculations

The hydration energy ΔE_{hyd} of Na^+ and Cl^- is obtained by the Lennard-Jones (LJ) potential energy and the Coulomb potential energy, which is contributed by each water-ion atomic pair. A simple box of TIP4P/EW water containing individual Na^+ and Cl^-, respectively, was used to validate the hydrated energy of the ion in bulk water. A 10 ns simulation was conducted with each single ion in a 3 nm × 3 nm × 3 nm water box (containing 900 water molecules) at 298 K and 1 atm, controlled by the NPT ensemble. This simulation system has been validated for effectiveness and feasibility through comparison with previous studies.[8, 9] The values of ΔE_{hyd} for Na^+ and Cl^- were calculated by averaging the data of at least 10000 frames in a consecutive 5 ns during the simulation of reaching steady state.

C. Potential of mean force derivations and calculations under electric fields

In the present system, where an electric field and a pressure difference coexist during desalination, ion transport through sub-nanometer carbon nanotubes is governed by two distinct physical contributions: an equilibrium free-energy landscape shaped by water structuring and polarization, and externally driven forces that sustain flux and selectivity. To disentangle these contributions, we adopt the following three-step simulation framework:

(1) Equilibrium PMF without pressure difference and electric field. We first compute the potential of mean force (PMF) for ion translocation under equilibrium conditions in the absence of both pressure difference and electric field, establishing a reference free energy landscape for ion entry into the CNT.

(2) Equilibrium PMF with electric field applied exclusively to water molecules. We then perform independent equilibrium simulations in which a constant electric field is applied solely to water molecules, while ions experience no direct electric force, and no pressure difference is imposed. The PMF obtained in this step quantifies how electric field-induced water reorientation modifies the intrinsic free energy barrier, while preserving a well defined canonical ensemble.

(3) Non-equilibrium simulations under combined pressure difference and electric field. Finally, we conduct non-equilibrium molecular dynamics simulations in which both a pressure difference and an electric field are applied concurrently. In this regime, the pressure gradient and the electric forces acting directly on ions are treated as genuine driving forces that sustain transport, enabling quantitative assessment of ion flux, selectivity, and desalination performance.

General Hamiltonian formulation. We consider a classical many-body system composed of ions, water molecules, and a confining CNT. The full microscopic state is specified by phase-space variables:

$$\Gamma = (\boldsymbol{r}_i, \boldsymbol{p}_i)_{i=1}^{N} \tag{S3}$$

where $\boldsymbol{r}_i$ is position and $\boldsymbol{p}_i$ is the momentum of atom i, respectively. The reference Hamiltonian (no external driving) reads:

$$H_0(\Gamma) = \sum \frac{\boldsymbol{p}_i^2}{2m_i} + U_{int}(\{\boldsymbol{r}_i\}) \tag{S4}$$

where U_{int} includes ion–ion, ion–water, ion-CNT, water–water, water-CNT interactions.

In equilibrium, the system is described by the canonical distribution:

$$\rho_0(\Gamma) = \frac{1}{Z_0} \exp\left[-\beta H_0(\Gamma)\right] \tag{S5}$$

$$Z_0 = \int d\Gamma \exp(-\beta H_0(\Gamma)) \tag{S6}$$

where $\beta = -k_B T$, k_B is is the Boltzmann constant and T indicates the temperature.

Potential of Mean Force as a constrained free energy. Let $z(\Gamma)$ be a reaction coordinate (e.g. the axial position of an ion along the CNT). The potential of mean force (PMF) is defined as:

$$PMF(z) = -k_B T \ln P(z) + C \tag{S7}$$

$$P(z) = \frac{1}{Z_0} \int d\Gamma \delta(z - z(\Gamma)) \exp(-\beta H_0(\Gamma)) \tag{S8}$$

This expression shows that the PMF is not a new Hamiltonian, but a conditional free energy, obtained by restricting the full accessible phase space to the hypersurface defined by z. The PMF therefore represents the free-energy landscape associated with a subset of the original phase space, rather than a modification of the underlying ensemble.

External electric field acting only on water molecules. We now introduce a uniform electric field $\boldsymbol{E}$ that couples exclusively to water molecules via their partial charges:

$$H_{E,w}(\Gamma) = H_0(\Gamma) - \sum_{j \in water} \boldsymbol{E} \cdot \boldsymbol{d}_j \tag{S9}$$

where $\boldsymbol{d}_j$ is the dipole moment of molecule j. Here we describe the interaction between water molecules and the electric field as the coupling of their instantaneous dipole moments, because each water molecule is electrically neutral as a whole:

$$\sum_{\alpha \in j} = q_{j\alpha} = 0 \tag{S10}$$

Write the atomic position of the water molecule j as:

$$\boldsymbol{r}_{j\alpha} = \boldsymbol{R}_j + \boldsymbol{\lambda}_{j\alpha} \tag{S11}$$

where $\boldsymbol{R}_j$ is the molecular reference point (e.g., the center of mass or the position of an oxygen atom), and $\boldsymbol{\lambda}_{j\alpha}$ is the relative displacement. Introducing the electric field term:

$$\sum_{\alpha \in j} q_{j\alpha} \boldsymbol{E} \cdot \boldsymbol{r}_{j\alpha} = \boldsymbol{E} \cdot (\boldsymbol{R}_j \sum_{\alpha} q_{j\alpha} + \sum_{\alpha} q_{j\alpha} \boldsymbol{\lambda}_{j\alpha}) \tag{S12}$$

where the first term is strictly zero due to the electroneutrality of water molecules, we obtain the potential energy term of the applied electric field $\boldsymbol{E}$ acting on water molecules:

$$U_{E,w} = -\sum_{\alpha \in j} q_{\alpha j} \boldsymbol{E} \cdot \boldsymbol{r}_{\alpha j} = -\sum_{\alpha \in j} q_{\alpha j} \boldsymbol{E} \cdot \boldsymbol{\lambda}_{\alpha j} = -\sum_{j \in water} \boldsymbol{E} \cdot \boldsymbol{d}_j \tag{S13}$$

The dipole coupling term satisfies the conditions that it is independent of particle velocity or time, and that the force is uniquely determined by, $\boldsymbol{F} = -\nabla_{\boldsymbol{r}} U_{E,w}$, for any generalized coordinate $\boldsymbol{r}$. Therefore, the system is still governed by a time-independent classical Hamiltonian Eq. S9.

The system admits a well-defined canonical distribution:

$$\rho_{E,w}(\Gamma) = \frac{1}{Z_{E,w}} \exp\left[-\beta H_{E,w}(\Gamma)\right] \tag{S14}$$

$$Z_{E,w} = \int d\Gamma \exp(-\beta H_{E,w}(\Gamma)) \tag{S15}$$

The corresponding PMF along z is:

$$PMF_{E,w}(z) = -k_B T \ln \int d\Gamma \ \delta(z_z(\Gamma)) \ \exp(-\beta H_{E,w}(\Gamma)) \tag{S16}$$

Thus, the electric field modifies the statistical weight of microstates through water orientation, while preserving equilibrium and the meaning of free energy.

Umbrella sampling under water-only electric field. Since the system remains in equilibrium, umbrella sampling method can be used for one-dimensional PMF calculations under water-only electric field. In windows of width 0.1 nm from z = -2.0 nm to z = 6.0 nm (beyond the CNT Center). Simulations were performed under consistent conditions, with a single ion harmonically restrained along the z-direction by a force constant of 10 kcal/mol/Å^2. After an initial 5 ns equilibration period to achieve steady-state fluid flow, the final 5 ns of data from each window were analyzed using the weighted histogram analysis method (WHAM) to determine the unbiased PMF. [10] To calculate the PMF profile of the ions, the space inside the window was divided into 100 bins.

To enhance sampling along z, a harmonic bias is introduced:

$$H^k(\Gamma) = H_{E,w}(\Gamma) + U^k_{bias} \tag{S17}$$

where U^k_{bias} is the biasing potential used in umbrella sampling to enforce the umbrella windows, typically represented as a harmonic potential:

$$U^k_{bias} = \frac{K}{2}(z(\Gamma) - z_k)^2 \tag{S18}$$

where z_k is the position of the kth biasing window and K is the force constant of the bias.

Each window k samples a biased distribution $p^k_b(\Gamma)$:

$$p^k_b(\Gamma) \propto \exp\left[-\beta H^k(\Gamma)\right] \tag{S19}$$

where $\beta = -k_B T$, k_B is is the Boltzmann constant and T indicates the temperature. Since the bias depends only on z, unbiased probabilities are recovered via standard reweighting, i.e., the WHAM:

$$p(z) = \frac{\sum_k n_k(z)}{\sum_k N_k \exp(-\beta \left[\frac{1}{2}K(z - z_k)^2 - f_k\right])} \tag{S20}$$

$$\exp(\beta f_k) = \int \exp(\beta U^k_{bias}(z))\ p(z)\ dz \tag{S21}$$

where $n_k(z)$ is in the kth window, the number of times the ion is sampled near the reaction coordinate z (usually referring to the bin interval where z is located), and N_k refers to the total number of sampled frames in the kth window, that is, the total number of all samples performed within the kth window. Finally, Eq. S20 and Eq. S21 are solved using an iterative procedure until convergence of $p(z)$ and f_k is achieved, after which the iteration is terminated. Thus, the unbiased PMF(z) can be calculated by the following expressions:

$$PMF(z) = -k_B T \ln \frac{\sum_k n_k(z)}{\sum_k N_k \exp(-\beta \left[\frac{1}{2}K(z - z_k)^2 - f_k\right])} \tag{S22}$$

We decompose the ion transport energy barrier into two distinct contributions: 1) The equilibrium component, which accounts for the modification of the free energy barrier due to water polarization under an electric field (captured by PMF); 2) The non-equilibrium component, arising from the enhancement of transport and selectivity due to external driving forces such as the electric field acting on ions and the pressure gradient. This decomposition guarantees that each observable quantity is rigorously associated with a statistically defined ensemble.

D. Molecular orientation analyses

The orientation of confined water molecules was evaluated by the angle $\theta_{dipole-z}$ between the dipole direction of a single water molecule and the axial direction of the CNTs. The dipole moment vector is defined as oriented from the region of negative charge to the region of positive charge. So, in water molecules, the dipole moment points from the oxygen atom toward the midpoint between the two hydrogen atoms. The axial direction of the CNTs is defined as the positive z-axis direction of the CNTs.

II. TABLE

TABLE I. Hydration energy for each ion in bulk water

Hydration free energy ΔE_{hyd} (kcal/mol)	Na^+	Cl^-
Experimental studies	-98.2[9]	-81.3[11]
Computed studies	-89.0[12]	-89.2[12]
This work	-91.5	-89.2

III. FIGURES

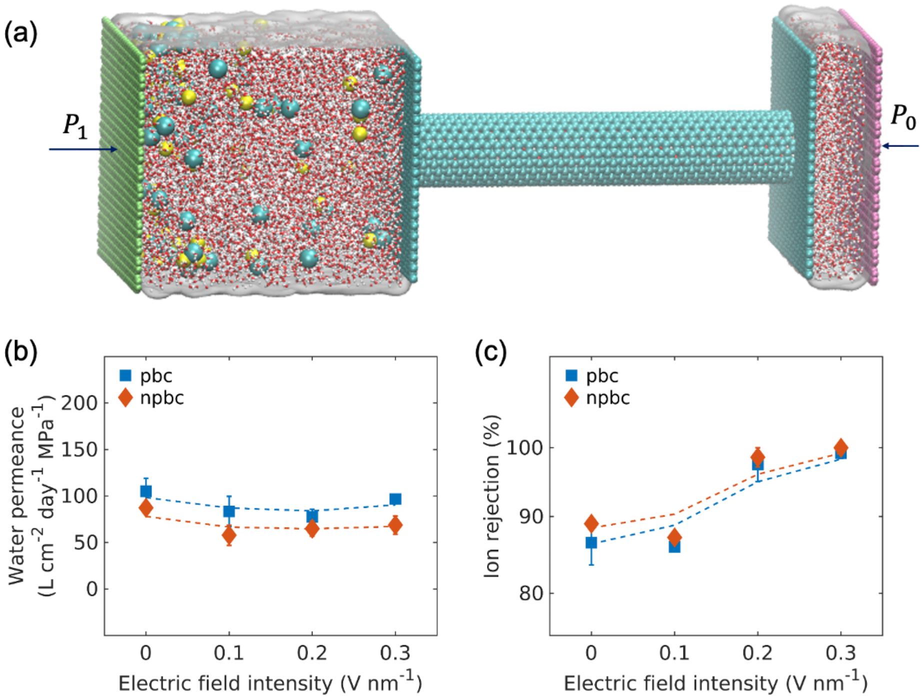

Fig. S2. Water desalination performed by validate models. (a) Desalination model with the non-periodic boundary condition (npbc). (b) Water permeance within CNT(11, 11) as a function of electric fields. (c) Ion rejection within CNT(11, 11) as a function of electric fields.

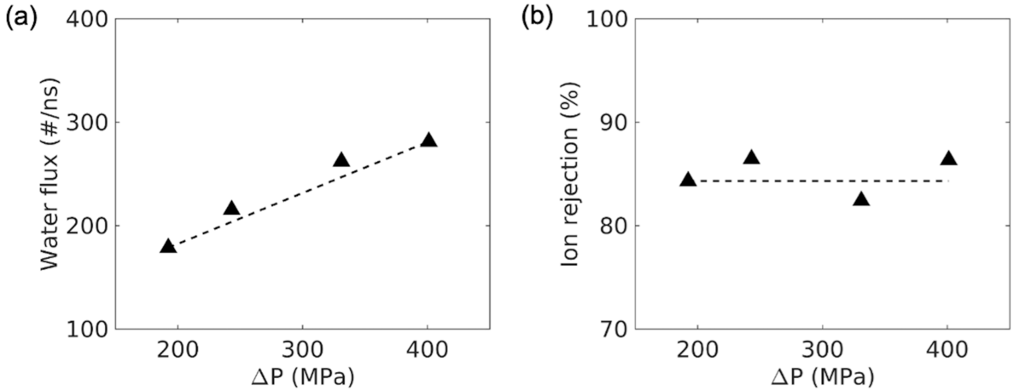

Fig. S3. Water desalination performance under different pressures ΔP without applying the electric field. (a) Linear relation between the water flux and pressure for CNT(11, 11). (b) Almost invariant ion rejection in CNT(11, 11) as the function of ΔP.

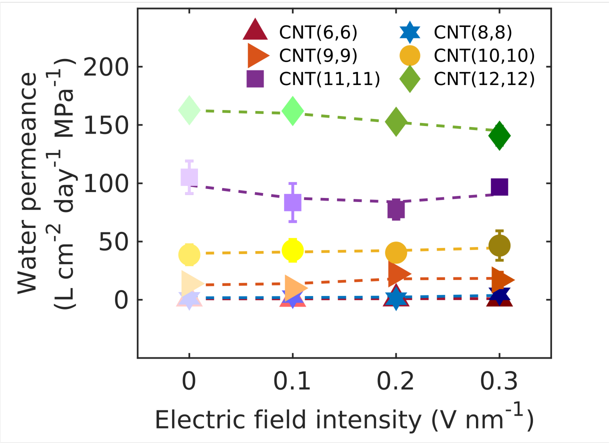

Fig. S4. Water permeance within CNTs of varying chirality as a function of electric fields.

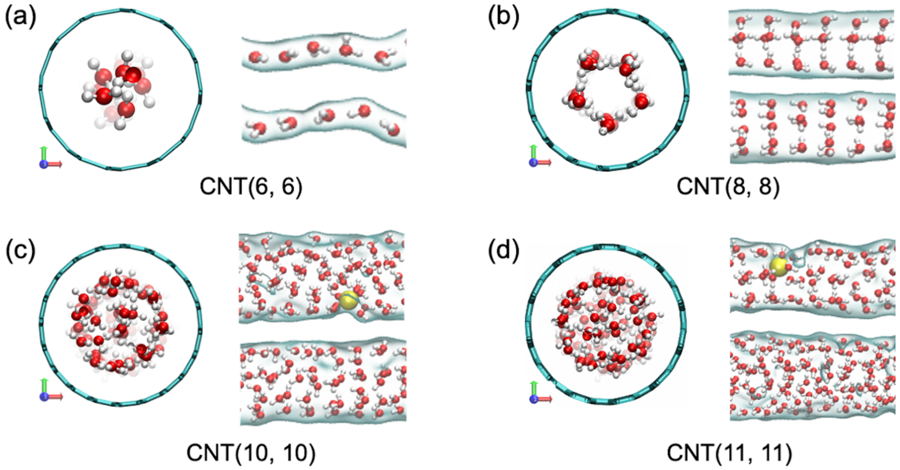

Fig. S5. Snapshots of water cross sections (left) and side view (right) for salt water confined in the CNTs. The side view on the top right shows the system at $E = 0$ V nm^{-1}, and the bottom right shows the system at $E = 0.3$ V nm^{-1}. (a) Single-file in CNT(6, 6), (b) single layer in CNT(8, 8), complex layered and bulk-like structure in (c) CNT(10, 10), (d) and CNT(11, 11).

[1] Y. Gao, M. Li, H. Zhang, Y. Zhang, W. Lu, and B. Xu, Anomalous solid-like necking of confined water outflow in hydrophobic nanopores, Matter **5**, 266 (2022).

[2] S. Joseph and N. Aluru, Why are carbon nanotubes fast transporters of water?, Nano Letters **8**, 452 (2008).

[3] A. Sam, S. K. Kannam, R. Hartkamp, and S. P. Sathian, Water flow in carbon nanotubes: The effect of tube flexibility and thermostat, The Journal of Chemical Physics **146** (2017).

[4] M. Heiranian and N. R. Aluru, Nanofluidic transport theory with enhancement factors approaching one, ACS Nano **14**, 272 (2019).

[5] J. A. Thomas and A. J. McGaughey, Water flow in carbon nanotubes: transition to subcontinuum transport, Physical Review Letters **102**, 184502 (2009).

[6] M. K. Borg, D. A. Lockerby, and J. M. Reese, A hybrid molecular-continuum simulation method for incompressible flows in micro/nanofluidic networks, Microfluidics and Nanofluidics **15**, 541 (2013).

[7] H. Li, Z. Ge, M. Aminpour, L. Wen, and S. A. Galindo-Torres, Pressure-dependent flow enhancement in carbon nanotubes, The Journal of Chemical Physics **160** (2024).

[8] L. A. Richards, A. I. Schäfer, B. S. Richards, and B. Corry, The importance of dehydration in determining ion transport in narrow pores, Small **8**, 1701 (2012).

[9] C. S. Babu and C. Lim, Theory of ionic hydration: Insights from molecular dynamics simulations and experiment, The Journal of Physical Chemistry B **103**, 7958 (1999).

[10] S. Kumar, J. M. Rosenberg, D. Bouzida, R. H. Swendsen, and P. A. Kollman, The weighted histogram analysis method for free-energy calculations on biomolecules. i. the method, Journal of Computational Chemistry **13**, 1011 (1992).

[11] Y. Marcus, Thermodynamics of solvation of ions. part 5.—gibbs free energy of hydration at 298.15 k, Journal of the Chemical Society, Faraday Transactions **87**, 2995 (1991).

[12] I. S. Joung and T. E. Cheatham III, Determination of alkali and halide monovalent ion parameters for use in explicitly solvated biomolecular simulations, The Journal of Physical Chemistry B **112**, 9020 (2008).